This paper describes objective technical results and analysis. Any subjective views or opinions that might be expressed in the paper do not necessarily represent the views of the U.S. Department of Energy or the United States Government.

Uncertainty Quantification in LES Computations of Turbulent Multiphase Combustion in a Scramjet Engine

SAND2017-9144C

– ScramjetUQ –

H. Najm[1], B. Debusschere[1], C. Safta[1], K. Sargsyan[1], X. Huan[1], J. Oefelein[1], Z. Vane[1], M. Eldred[2], G. Geraci[2], O. Knio[3], I. Sraj[3], G. Scovazzi[3], O. Colomés[3], Y. Marzouk[4], O. Zahm[4], F. Menhorn[4], R. Ghanem[5], and P. Tsilifis[5]

[1]Sandia National Laboratories, Livermore, CA
[2]Sandia National Laboratories, Albuquerque, NM
[3]Duke University, Durham, NC
[4]Massachusetts Institute of Technology, Cambridge, MA
[5]University of Southern California, Los Angeles, CA

Quarterly DARPA Review Telecon

andia National Laboratories is a multimission laboratory managed and operated by National Technology & Engineering Solutions of Sandia, LLC, a wholly own subsidiary of Honeywell International Inc., for the U.S. Department of Energy's National Nuclear Security Administration under contract DE-NA0003525.

Outline

ScramjetUQ Project Team

Current team includes Sandia (CA+NM), Duke, MIT, and USC.

Institution	Expertise	Participants
Sandia	UQ + Comb	**Habib Najm**, Bert Debusschere, Cosmin Safta, Khachik Sargsyan Xun Huan
	LES + SprayComb	Joe Oefelein (now at Georgia Tech)
	UQ + Optim	Mike Eldred, Gianluca Geraci
Duke	UQ + Comb	**Omar Knio**, Ihab Sraj
	LES	Guglielmo Scovazzi, Oriol Colomés
MIT	UQ + Optim	**Youssef Marzouk**, Olivier Zahm, Friedrich Menhorn
USC	UQ + Optim	**Roger Ghanem**, Panagiotis Tsilifis

Outline

Phase I Achievements

- Dimensionality reduction in P1
  - GSA, CS-PCE regression, ML/MF
    - Identified 6 important parameters
  - Established utility of ML/MF in this system
  - Established utility of BA/Manifolds in this system
  - Inverse problem dimensionality reduction
- OUU demonstration in P1
  - OUU algorithms
  - OUU software infrastructure
  - Coupling Dakota, SNOWPAC, RAPTOR

GSA dimensionality reduction – Phase 1

GSA via PCE-Sparse Regression and ML/MF

- Applied Global Sensitivity Analysis (GSA) to P1
  - Sparse Polynomial Chaos surrogates via ℓ_1-norm min
  - Solution methods for sparse regression and techniques to avoid overfitting (*manuscript submitted to SIAM/ASA-JUQ*)
  - Under either ML or MF

  to identify important P1 parameters

Result

Identified 6 dominant parameters for relevant LES QoIs in P1

MLMF dimensionality reduction – Phase 1

- **Main Goal:** Variance reduction (improved estimator reliability) for a limited number of HF simulation by adding a 'large' number of LF realizations

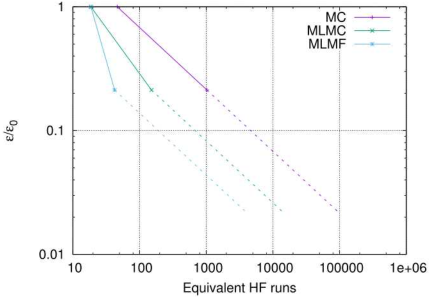

Aggressive Samples redistribution (P1 with 24D):

- 3D LES: **9 fine** + 263 coarse
- 2D LES: 68 fine + 4191 coarse

Extremely high computational cost

	2D	3D
$d/8$	1	204
$d/16$	25.5	1844

- More challenging to obtain variance reduction by ML for **high turbulence cases**

- Non monotonic **RMS** variance decay
- Need for managing **spatial/time resolutions** in a unified fashion

	$P_{0,mean}$	$P_{0,rms,mean}$	M_{mean}	TKE_{mean}	χ_{mean}
			P1		
$d/8$	4.025e-03	1.905e-06	1.992e-02	3.349e-07	4.245e-03
$d/16$	4.033e-07	7.778e-08	6.690e-05	1.748e-08	4.400e-05
			P1 updated		
$d/8$	4.058e-03	1.906e-06	1.600e-02	7.533e-07	9.414e-04
$d/16$	2.850e-04	7.370e-07	2.076e-03	2.997e-07	2.574e-02

- **Integration** of the ML/MLMF strategy into the **OUU** loop (Dakota/SNOWPACK)

BA/Manifolds dimensionality reduction – Phase 1

Dimension reduction is achieved both via "learned" subspaces via projections and "learned" manifolds via sampling:

Subspace detection in PCE permits concentration of L_2 projections:

- Convergent stochastic approximations are accelerated in the transformed coordinates.
- Maintain accuracy and functional form for use in sensitivity calculations and optimization.
- Numerical cost is proportional to stochastic dimension.

Diffusion manifold detection permits concentration of samples:

- Samples scattered around manifold have smaller variance than samples scattered in ambient space.
- Structure of manifold is better delineated with more stochastic parameters; thus requiring fewer samples to characterize QoI.

Inverse problem dimensionality reduction – Phase 1

Dimension reduction is necessary for inference in large-scale and computationally intensive problems, enabling:

- Accelerated sampling
- Construction of reduced/surrogate models

Covariance-based (non-intrusive) estimation of data-informed directions

- Sample size/detection limits from **asymptotic theory** of "spiked" covariance matrices
- Application to RAPTOR P1 problem

New gradient-based method (intrusive) for certified dimension reduction

- Provides **rigorous control** of error (Kullback-Leibler divergence)
- Outperforms previous dimension reduction methods for Bayesian inverse problems

OUU Algorithms – Phase 1

Algorithms & infrastructure:

- Dakota trust region model management (TRMM):
  - TRMM incorporates multilevel-multifidelity in simulation, UQ, both
  - Leverage RAPTOR model forms {2D, 3D} + discretizations {d/8, d/16}
  - Recursions for deep hierarchies (beyond bi-fidelity)
- (S)NOWPAC derivative-free opt: deterministic/stochastic solvers
  - NOWPAC $\rightarrow$ SNOWPAC: adapt TR to noise, GP's to mitigate noise, efficient GP regression via low rank approx (SoR, DTC, FITC)
  - Performance eval against other common DFO solvers
- Integration of (S)NOWPAC + Dakota
  - `NOWPACOptimizer`: solver spec, input var transforms, constraint mappings, final result logging, parallel config
  - Abstract error est. in `Iterator`, `Model`: std errors in MC, MLMC stats
  - Phase II target for P2 OUU: SNOWPAC + MLMC

OUU Software Framework – Phase 1

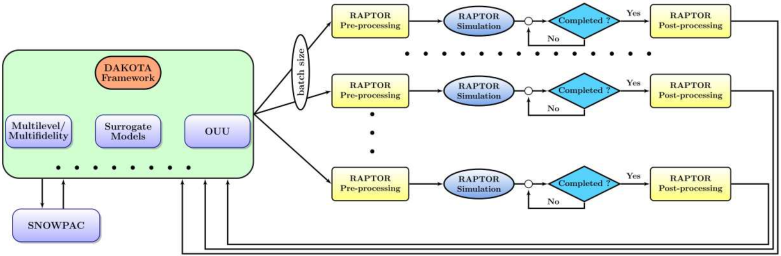

(DAKOTA+SNOWPAC) – RAPTOR Interface

- RAPTOR black box driver based on system/fork + file I/O
- Asynchronous local concurrency with work directories
- Detection and mitigation of failed simulations (e.g., residual divergence, node failure)
- Up to 3 levels of parallelism: optimizer, UQ, RAPTOR

OUU Demo – Phase 1

P1 (jet-in-crossflow) deployments:

- PCBDO w/ combined exp: reuse of 2D/3D GSA data sets

Model	$\hat{\phi}$	Initial $\mathbb{E}[\chi]$	Initial $\mathbb{E}[\phi]$	Final $\mathbb{E}[\chi]$	Final $\mathbb{E}[\phi]$	Iter
2D	.06	3.480e-1	6.356e-2	3.229e-1	6.000e-2	3
3D	.013	1.377e-3	1.392e-2	1.212e-3	1.300e-2	2

- Multifidelity TRMM with UQ/simulation resolutions

Iteration	$\mathbb{E}[\phi]$	$\mathbb{V}^{\frac{1}{2}}[\phi]$	$\mathbb{E}[\chi]$	Trust region ratio
0	1.142e-01	5.800e-03	9.848e-02	N/A
1	1.074e-01	5.646e-03	8.832e-02	1.443
2	1.003e-01	5.390e-03	7.790e-02	1.497

- SNOWPAC closed-loop coupling with RAPTOR P1 code

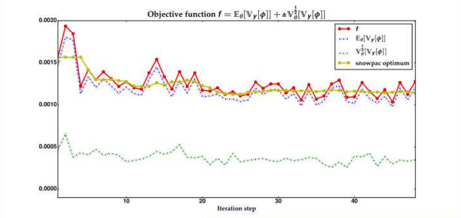

Outline

Phase II Research Goals

- Establish routine computations with full scramjet P2 code
- Identify reduced dimensional uncertain parameter space for P2
    - GSA, PC/CS regression, MLMF, BA/Manifolds
- Demo reduced dimensional Bayesian inversion with P2
- Demo model and mesh error estimation in P2
- Demo OUU with P2 following WPAFB metrics

Phase II Progress

- LES code
- Forward UQ and dimensionality reduction
  - GSA PC/CS, MLMF
  - Basis Adaptation/Manifolds
- Bayesian inversion and dimensionality reduction
- Model Error
- Mesh Error
- OUU

Outline

1. Phase-I Major Achievements
2. Phase-II Progress
   - Application Code – Scramjet
   - High Dimensionality
   - Basis Adaptation & Manifold Sampling
   - Bayesian Inference
   - Model Error
   - Mesh Discretization Error
   - Optimization under Uncertainty
3. Closing Remarks

LES Code Highlights – HIFiRE Scramjet

What we've done

Multiscale-multiphysics application of Large Eddy Simulation (LES)

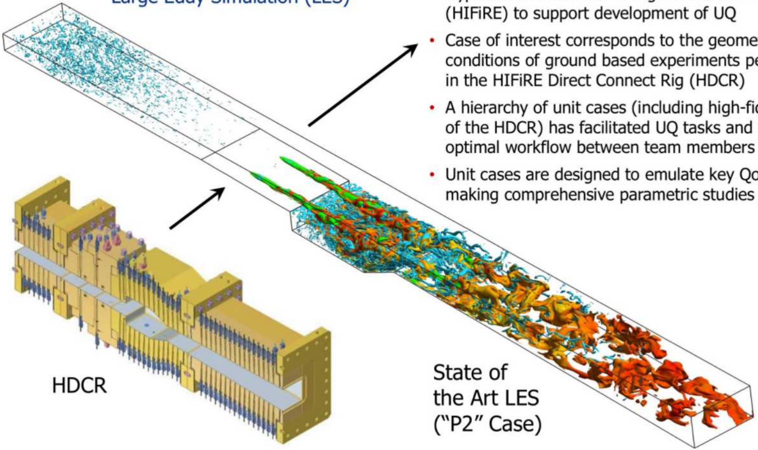

- Provided benchmark LES calculations of the Hypersonic International Flight Research Experiment (HIFiRE) to support development of UQ
- Case of interest corresponds to the geometry and conditions of ground based experiments performed in the HIFiRE Direct Connect Rig (HDCR)
- A hierarchy of unit cases (including high-fidelity LES of the HDCR) has facilitated UQ tasks and provided optimal workflow between team members
- Unit cases are designed to emulate key QoIs while making comprehensive parametric studies possible

LES Code Findings

What we've learned

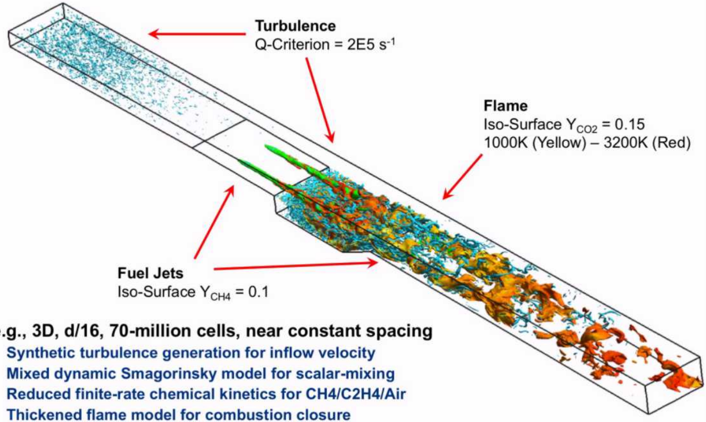

e.g., 3D, d/16, 70-million cells, near constant spacing

- **Synthetic turbulence generation for inflow velocity**
- **Mixed dynamic Smagorinsky model for scalar-mixing**
- **Reduced finite-rate chemical kinetics for CH4/C2H4/Air**
- **Thickened flame model for combustion closure**
- **ODE based wall-model for turbulent/thermal boundary layer**

- Established full 3D modeling of HIFiRE DCR configuration (P2) with complete system of sub-models validated for baseline conditions
- Established RAPTOR-Dakota software framework for OUU using P2

Detailed analysis of flow has provided insights into local processes

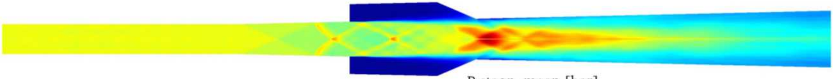

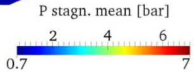

Mean stagnation pressure loss
Instantaneous flow characteristics

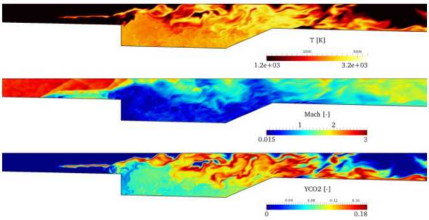

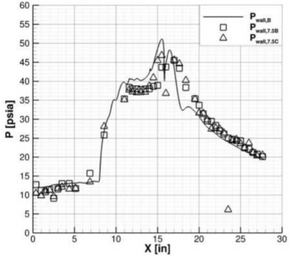

Pressure distribution along wall

RAPTOR I/O has been instrumented to interface with Dakota and SNOWPAC

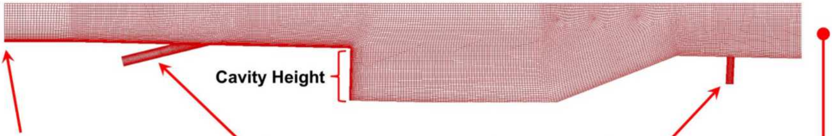

Inlet:
- Stagnation Pressure
- Stagnation Temperature
- Mach Number
- Turbulence Intensity
- Turbulence Length Scale
- Boundary Layer Thickness

Primary Injector:
- Equivalence Ratio
- Stagnation Temperature
- Mach Number
- Turbulence Intensity
- Turbulence Length Scale
- Axial Position
- Injection Angle

Secondary Injector:
- Equivalence Ratio
- Stagnation Temperature
- Mach Number
- Turbulence Intensity
- Turbulence Length Scale

Performance Metrics:
- Thermal Efficiency
- Phi-Burn (>= 0.7)
- Location of Leading Shock
- Bulk Loss in Stagnation Pressure
- Magnitude of Pressure Oscillations
- Combustion Chamber M > 1 (Scram Mode)

Application Impact

- Established hierarchy of computations of 2D/3D unit problem cases including the full 3D HIFiRE Scramjet configuration
  - Performed and analyzed over 8000 LES calculations required for development and testing of UQ tasks
  - Created interface between RAPTOR code and UQ routines via a shared repository and related pre- and post-processing scripts
- Combination of P1 and P2 calculations have provided progression of affordable unit cases that emulate key physics
  - P1 cases have facilitated testing and refinement of various UQ methods along with workflow required for data management and analysis
  - Full 3D P2 case provides the target reference case for application of the suite of UQ methodologies for both model and system optimization
- Demonstrated full set of physics sub-models in the full 3D P2 configuration at baseline conditions
  - Established RAPTOR-Dakota software interface for OUU with P2
  - Managed the balance between computational cost and fidelity (which will continue to be a leading challenge)

Outline

Hi-D Highlights

What we've done

Software Infrastructure

- Adapted DAKOTA – RAPTOR software connection infrastructure for the GSA effort
  - Sampling for GSA studies is now driven by DAKOTA −tolerant to faults
  - Adaptive Sparse Quadrature currently run in either ML or MF mode

GSA/ASQ progress

- Applied Global Sensitivity Analysis (GSA) to P2 in an ML context
  - Sparse Polynomial Chaos surrogates via ℓ_1-norm min
- Algorithm development in progress for MF/ML ASQ
  - provide optimal quadrature adaptation across models of different fidelity and levels
  - balance improvement of overall surrogate and computational costs

Hi-D Findings

What we've learned

GSA

- Completed set of simulations for P2 2D with coarse ($\delta = d/8$) and intermediate ($\delta = d/16$) grid resolutions
  - 11 uncertain parameters; design variables fixed at nominal values
  - Inlet Mach number and temperature were the dominant parameters for a set of QoIs investigated in this preliminary study
- Preliminary results for 2D P2 configuration indicate longer time horizons needed to reach near-stationary state dynamics

ASQ

- Single fidelity ASQ results completed for P2 2D coarse grid
- MF development in progress

Hi-D Progress: GSA for P2

Setup

- QoIs: thermal efficiency ($\eta_{thermal}$), stagnation pressure loss (ΔP_{stag}), and mean TKE at $x/d = 190$ (right after the 2nd set of injectors)
- 256 simulations for $d/8$ and 172 simulations for $d/16$

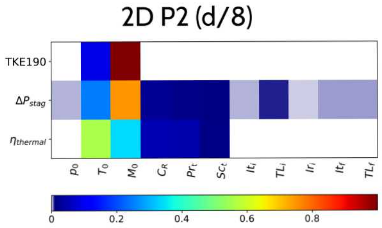

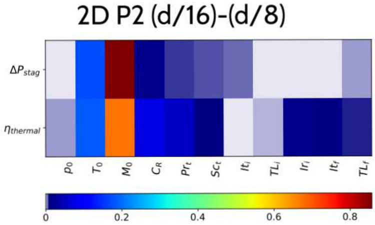

Result

Inlet Mach number (M_o) and stagnation temperature (T_o) are the dominant parameters for 2D P2 case.

Hi-D Progress: Adaptive Sparse Quadrature for P2

- PCE approximation constructed via 3 level adaptive sparse quadrature
  - the design adapted to primarily include the important directions

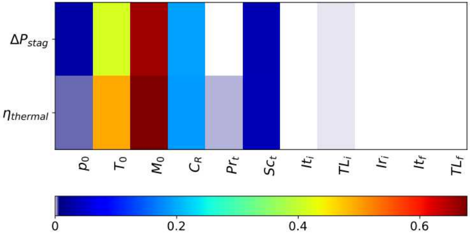

- Results are similar to GSA via sparse regression; some turbulence models parameters (C_R) exhibit increased importance
- Work in progress to include balance between cost and accuracy in the MF design.

Outline

Basis Adaptation Highlights

What we've done

Main Idea

- Orthogonal polynomials are constructed with respect to rotated germ, and then truncated for enhanced compression.
- The adaptation isometry is now additionally constrained with statistical (samples, likelihood) and orthogonality (sensitivity ranking of initial dimensions) information.
- The result is more concentration of QoI around dominant directions.

Analysis

- Convergence criteria and assurance in adapted directions
- Error analysis with respect to errors in isometry evaluation
- Adaptation interpolated across models,
  refinements,
  and design space

Basis Adaptation Highlights

What we've done

Main Idea

- Orthogonal polynomials are constructed with respect to rotated germ, and then truncated for enhanced compression.
- The adaptation isometry is now additionally constrained with statistical (samples, likelihood) and orthogonality (sensitivity ranking of initial dimensions) information.
- The result is more concentration of QoI around dominant directions.

Analysis

- Convergence criteria and assurance in adapted directions
- Error analysis with respect to errors in isometry evaluation
- Adaptation interpolated across models,
  refinements,
  and design space

Manifold Sampling Highlights

What we've done

Main Idea

- An implicit manifold is "learned" from a handful of initial samples.
- Statistical analysis and sampling are conducted around this manifold, exhibiting smaller scatter than would otherwise be observed.
- A projected Itô equation is constructed to sample directly on this manifold.
- Joint density of Objective function, design variables, uncertain parameters is pre-computed for real-time optimization.

Analysis

- Convergence criteria and assurance for learning process
- Statistical selection criteria for diffusion kernels

Manifold Sampling Highlights

What we've done

Main Idea

- An implicit manifold is "learned" from a handful of initial samples.
- Statistical analysis and sampling are conducted around this manifold, exhibiting smaller scatter than would otherwise be observed.
- A projected Itô equation is constructed to sample directly on this manifold.
- Joint density of Objective function, design variables, uncertain parameters is pre-computed for real-time optimization.

Analysis

- Convergence criteria and assurance for learning process
- Statistical selection criteria for diffusion kernels

Basis Adaptation via Compressive Sensing

- ℓ_1 minimization for PCE with rotated basis
  Compute jointly the coefficients $\tilde{c}_\beta$ and isometry $\mathbf{A}$ for

$$u := u(\boldsymbol{\eta}) = \sum_{\boldsymbol{\beta} \in \mathcal{J}_Q^d} \tilde{c}_{\boldsymbol{\beta}} \psi_{\boldsymbol{\beta}}(\boldsymbol{\eta}) = \sum_{\boldsymbol{\beta} \in \mathcal{J}_Q^d} \tilde{c}_{\boldsymbol{\beta}} \psi_{\boldsymbol{\beta}}(\mathbf{A}\boldsymbol{\xi}) \qquad (1)$$

  by finding

$$(\mathbf{c}^*, \mathbf{A}^*) = \arg\min_{\mathbf{c},\mathbf{A}} \left\{ \frac{1}{2\sigma^2} ||\mathbf{u} - \Psi_{\mathbf{A}}\mathbf{c}||_2^2 + \lambda ||\mathbf{c}||_1 \right\}. \qquad (2)$$

- Example: We solve (2) for a 1d, 2d & 3d adaptation of the u-velocity component averaged along the y-profile (P2 domain - $x/d = 220$). Left to right: log-likelihood, chaos coefficients & 2d PCE manifold

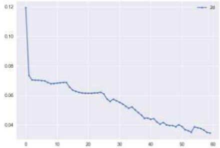

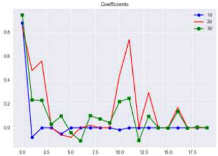

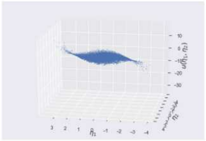

Manifold Sampling for PDF and Extremes

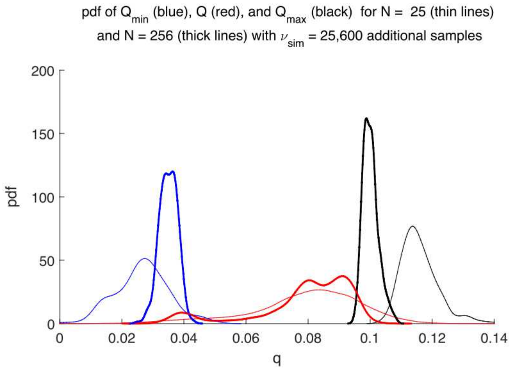

Probability of Thermal Efficiency with Minimum and Maximum.

Manifold Sampling for PDF and Extremes

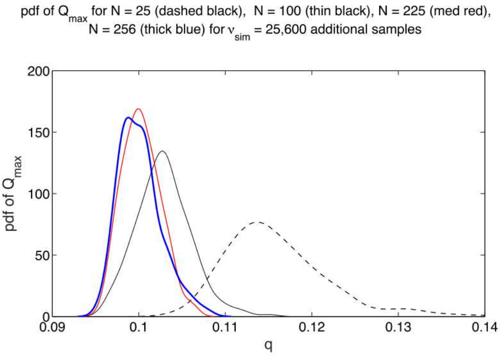

Probability of Maximum of Thermal Efficiency: Convergence with learning.

Manifold Sampling for PDF and Extremes

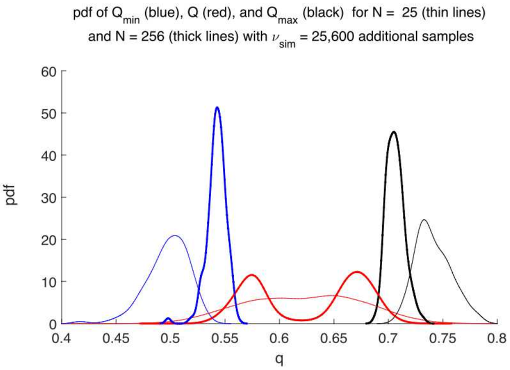

Probability of Pressure Stagnation Loss, with Minimum and Maximum.

Manifold Sampling for PDF and Extremes

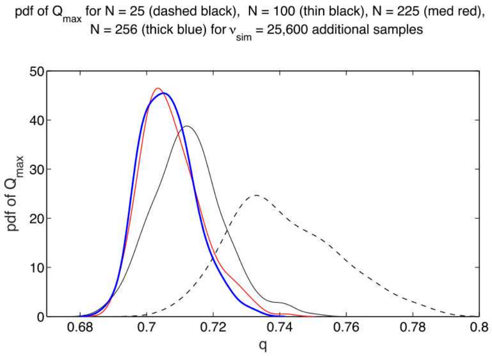

Probability of Pressure Stagnation Loss: Convergence with learning.

Basis Adaptation and Manifold Sampling Impact

Basis Adaptation

Computational cost is less than linear in stochastic dimension without loss of accuracy.

Manifold Sampling

- Summarize a large dataset with a data-driven generator
- Augment a small dataset by conditioning on intrinsic structure

Basis Adaptation and Manifold Sampling Impact

Basis Adaptation

Computational cost is less than linear in stochastic dimension without loss of accuracy.

Manifold Sampling

- Summarize a large dataset with a data-driven generator
- Augment a small dataset by conditioning on intrinsic structure

Outline

Bayesian Inference – Highlights

What we've done

Goal: reduce the dimensionality of Bayesian inverse problems:

$$\pi_{\text{pos}}(x) \propto \mathcal{L}(x)\pi_{\text{pr}}(x) \quad \text{with} \quad x \in \mathbb{R}^d, d \gg 1$$

Methodology:

- Start with a **best approximation problem** for the posterior distribution
- Derive an **upper bound** for the error (KL-divergence)
- Minimize the upper bound using **principal component analysis (PCA)** of the gradient of the log-likelihood

Highlights (Phase II)

- Rigorous analysis of the approximation schemes
  - Number of gradient evaluations for certified dimension reduction
  - Approximation scheme for conditional expectations
- Successfully tested on numerical benchmarks

Bayesian Inference – Findings

What we've learned

Dimension reduction problem: find an approximation of π_{pos} of the form

$$\tilde{\pi}_{\text{pos}}(x) \propto \widetilde{\mathcal{L}}(P_r x)\ \pi_{\text{pr}}(x) \quad \text{where} \quad \begin{cases} P_r \in \mathbb{R}^{d\times d} \text{ is a rank-}r \text{ projector} \\ \widetilde{\mathcal{L}} \text{ is a positive function} \end{cases}$$

Ideal algorithm

1. Compute
$$H = \int \nabla \log \mathcal{L} \otimes \nabla \log \mathcal{L}\ \mathrm{d}\pi_{\text{pos}}$$
2. Define P_r as the projector onto the dominant eigenspace of H
3. Compute the conditional expectation
$$\widetilde{\mathcal{L}}(P_r x) = \mathbb{E}_{\pi_{\text{pr}}}(\mathcal{L} | P_r x)$$

Certified control of the error with the eigenvalues λ_i of H:

$$D_{\text{KL}}(\pi_{\text{pos}} || \tilde{\pi}_{\text{pos}}) \leq \frac{1}{2} \sum_{i>r} \lambda_i$$

Bayesian Inference Progress – Details

- Monte Carlo approximation of H

$$H \approx \frac{1}{K}\sum_{i=1}^{K} \nabla \log \mathcal{L}(X_i) \otimes \nabla \log \mathcal{L}(X_i) \quad \text{with} \quad X_i \overset{\text{iid}}{\sim} \pi_{\text{pos}}$$

Proposition

Under some assumptions, **quasi-optimal projectors** are obtained with high probability $1-\delta$ if

$$K \geq \mathcal{O}\left(\sqrt{\text{rank}(H)} + \sqrt{\log(2\delta^{-1})}\right)^2$$

- Approximation of the conditional expectation

$$\mathbb{E}_{\pi_{\text{pr}}}(\mathcal{L}|P_r x) \approx \mathcal{L}(P_r x + (I_d - P_r)Y) \quad \text{with} \quad Y \sim \pi_{\text{pr}}$$

Proposition

The random distribution $\widetilde{\pi}_{\text{pos}}$ satisfies

$$\mathbb{E}\left(D_{\text{KL}}(\pi_{\text{pos}} \,||\, \widetilde{\pi}_{\text{pos}})\right) \lesssim \Omega \sum_{i>r} \lambda_i$$

Bayesian Inference Progress – Details

- Monte Carlo approximation of H

$$H \approx \frac{1}{K} \sum_{i=1}^{K} \nabla \log \mathcal{L}(X_i) \otimes \nabla \log \mathcal{L}(X_i) \quad \text{with} \quad X_i \overset{\text{iid}}{\sim} \pi_{\text{pos}}$$

Proposition

Under some assumptions, **quasi-optimal projectors** are obtained with high probability $1 - \delta$ if

$$K \geq \mathcal{O}\left(\sqrt{\text{rank}(H)} + \sqrt{\log(2\delta^{-1})}\right)^2$$

- Approximation of the conditional expectation

$$\mathbb{E}_{\pi_{\text{pr}}}(\mathcal{L}|P_r x) \approx \mathcal{L}(P_r x + (I_d - P_r)Y) \quad \text{with} \quad Y \sim \pi_{\text{pr}}$$

Proposition

The random distribution $\widetilde{\pi}_{\text{pos}}$ satisfies

$$\mathbb{E}\left(D_{\text{KL}}(\pi_{\text{pos}} \,||\, \widetilde{\pi}_{\text{pos}})\right) \lesssim \Omega \sum_{i>r} \lambda_i$$

Bayesian Inference Progress – Details

Identify the coefficient field κ of the Poisson equation

$$-\nabla \cdot \kappa \nabla p = f$$

from pointwise observations:

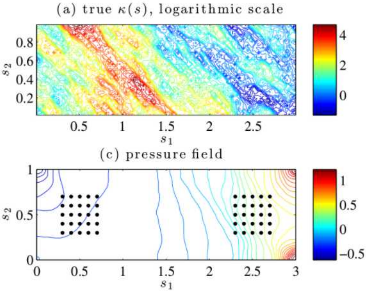

$$D_{\mathsf{KL}}(\pi_{\mathsf{pos}} || \tilde{\pi}_{\mathsf{pos}}) = f(r)$$

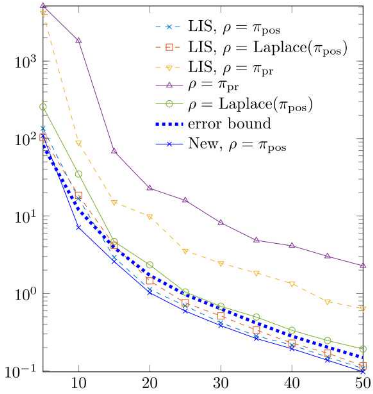

$$\mathbf{H}^{(\rho)} = \int \nabla \log \mathcal{L} \otimes \nabla \log \mathcal{L} \, \mathsf{d}\rho$$

$$\mathbf{H}_{\mathsf{LIS}}^{(\rho)} = \int (\nabla G)^T \Gamma_{\mathsf{obs}}^{-1} (\nabla G) \, \mathsf{d}\rho$$

Bayesian Inference – Impact

Key impacts:

- New understanding of dimension reduction methods for **nonlinear and non-Gaussian** Bayesian inverse problems
  - Replaces previous heuristics whose approximation properties, relative to an *optimal* approximation, were not understood
- **Certified/computable bounds** on the error in a posterior approximation
- New methodology: **more effective dimension reduction** than either the LIS or the AS!
- More efficient **computation:**
  - Samplers guided by the data-informed subspace
  - Surrogate modeling on the data-informed subspace (essential for RAPTOR P2)

Outline

Model Error: method and features

Embedded model error: (Sargsyan, Najm, Ghanem, 2015)

$$g_i \approx f_i(\lambda + \delta)$$

- Embeds model error in specific submodel phenomenology
- Allows *targeted* placement of model error term (e.g., in locations where key modeling assumptions and approximations are made)
- Respects physical constraints and governing equations by definition
- Allows meaningful extrapolation to other QoIs
- Disambiguates model error from data noise

- Automated approach to calibrate low-fidelity models with high-fidelity data
- Variance-based attribution of overall predictive uncertainty - data noise, surrogate construction, model error, calibration (i.e. posterior)
- Developed workflow for model error representation, quantification and propagation; Inference library in UQTk v3.0 (www.sandia.gov/uqtoolkit)
- Used Bayesian model selection to select parameters for model error embedding

Model Error – wall model LES

- Wall model formulation by [Kawai and Larsson, 2012]: equilibrium boundary layer assumption, ODE w.r.t. wall-normal coordinate.
- Initial tests on a simple channel flow.
- Key challenge: a discrete parameter m_{wm}.
- Built a 3-parameter surrogate for $m_{wm} = 25$, using 250 wall-model enabled LES simulations.
- Wall model parameter calibration, with embedded model error, using baseline data with background grid only (i.e., wall-model turned off).

Parameter	Range	Nominal	Description
BL_i	$[8.5, 34.0] \times 10^{-3}$ m	17.0×10^{-3} m	Inlet boundary layer thickness
L_{wm}	$[0.01, 0.25]$	0.05	Fraction of the inlet boundary layer thickness to use for wall-model
d_{wm}	$[0.01, 0.1]$	0.03	Fraction of the first LES grid cell as initial spacing for the embedded mesh
m_{wm}	$\{5, 15, 25, 35\}$	25	Number of grid points to use in embedded mesh

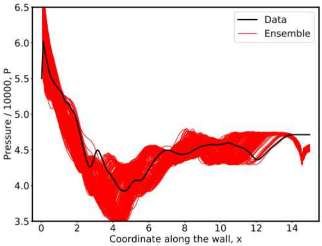

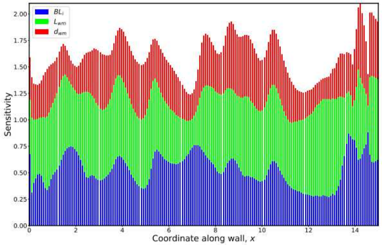

Model Error – wall model LES

- Wall model formulation by [Kawai and Larsson, 2012]: equilibrium boundary layer assumption, ODE w.r.t. wall-normal coordinate.
- Initial tests on a simple channel flow.
- Key challenge: a discrete parameter m_{wm}.
- Built a 3-parameter surrogate for $m_{wm} = 25$, using 250 wall-model enabled LES simulations.
- Wall model parameter calibration, with embedded model error, using baseline data with background grid only (i.e., wall-model turned off).

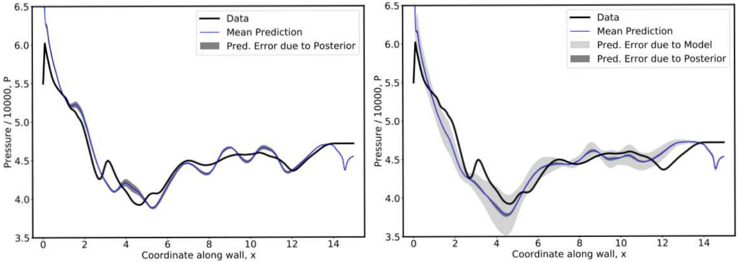

Overall uncertainty breakdown for posterior predictive:

$$\sigma_i^2 = \underbrace{\mathbb{E}_{\tilde{\lambda}}\left[\sigma_i^2(\tilde{\lambda})\right]}_{\text{Model error}} + \underbrace{\mathbb{V}_{\tilde{\lambda}}\left[\mu_i(\tilde{\lambda})\right]}_{\text{Posterior uncertainty}} + \underbrace{(\sigma_i^{LOO})^2}_{\text{Surrogate error}} + \underbrace{(\sigma_{f_i})^2}_{\text{Data noise}}$$

Model Error: discrete/categorical parameters

- We have developed an approach to incorporate discrete parameters in the embedded model error framework.
- Augment discrete parameters with a probability mass function (PMF) and infer the mass weights (just like the continuous case of inferring PDF).
- Allows MCMC on continuous parameters.
- Connections to Bayesian model averaging and model selection.

The overall mean for a given (α, a, x) is

$$\mu(\alpha, a; x) = \mathbb{E}_{\Lambda,L}\left[f(\Lambda(\alpha), L(a); x)\right] = \sum_{r=1}^{R} a_r \mu_r(\alpha; x),$$

and the variance is

$$\begin{aligned}\sigma^2(\alpha, a; x) &= \mathbb{V}_{\Lambda,L}\left[f(\Lambda(\alpha), L(a); x)\right] \\ &= \underbrace{\sum_{r=1}^{R} a_r \sigma_r^2(\alpha; x)}_{\text{due to cont. param.}} + \underbrace{\sum_{r=1}^{R} a_r \mu_r^2(\alpha; x) - \mu(\alpha, a; x)^2}_{\text{due to categorical param.}}.\end{aligned}$$

Model Error: optimal embedding via Bayes factors

- Which parameters should be augmented with stochastic structure to capture model error?
- Bayes' formula for a given model M_k

$$\overbrace{p(\tilde{\lambda}|y, M_k)}^{\text{Posterior}} = \frac{\overbrace{p(y|\tilde{\lambda}, M_k)}^{\text{Likelihood}}\,\overbrace{p(\tilde{\lambda}|M_k)}^{\text{Prior}}}{\underbrace{p(y|M_k)}_{\text{Evidence}}}$$

- Bayes factor: ratio between evidence terms of two models
- Model evidence is a high-dimensional integral, requiring many model evaluations – challenging to compute
- We investigated different numerical methods
  - GA (Gaussian approximation to posterior)
  - HM (Harmonic Mean estimator)
  - MC (Plain Monte-Carlo)
  - IMC (Importance sampling Monte-Carlo)
  - TMCMC (Transitional Markov chain Monte-Carlo)

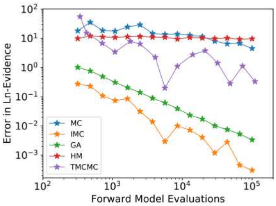

Model Error: summary

- Model error approach employs both **forward and inverse UQ** technologies
- Embedded model error allows meaningful predictions of full set of QoIs (i.e. extrapolating to QoIs not used for calibration)
- Informs LES modeling on the highest contributors to predictive uncertainty error budget
  - in most studies so far, model error overwhelms parametric uncertainty, surrogate errors, and data noise.
- Results using model error treatment capture discrepancy much better than results without model error treatment
- Allows replacement of expensive models with less expensive alternatives while quantifying the resulting model discrepancies
  - Huge computational savings via low-fidelity model (e.g. 2D-vs-3D) with augmented uncertainties

---

- All ingredients ready for model error assessment within P2

Model Error: summary

- Model error approach employs both **forward and inverse UQ** technologies
- Embedded model error allows meaningful predictions of full set of QoIs (i.e. extrapolating to QoIs not used for calibration)
- Informs LES modeling on the highest contributors to predictive uncertainty error budget
  - in most studies so far, model error overwhelms parametric uncertainty, surrogate errors, and data noise.
- Results using model error treatment capture discrepancy much better than results without model error treatment
- Allows replacement of expensive models with less expensive alternatives while quantifying the resulting model discrepancies
  - Huge computational savings via low-fidelity model (e.g. 2D-vs-3D) with augmented uncertainties

---

- **All ingredients ready for model error assessment within P2**

Outline

1. Phase-I Major Achievements
2. Phase-II Progress
   - Application Code – Scramjet
   - High Dimensionality
   - Basis Adaptation & Manifold Sampling
   - Bayesian Inference
   - Model Error
   - Mesh Discretization Error
   - Optimization under Uncertainty
3. Closing Remarks

Phase II Progress: Mesh Discretization Errors

We focused on extending the RF approaches developed in Phase I to non-reacting LES flow (RAPTOR) by:

1. Establishing MDE formulation for RAPTOR.
2. Demonstrating MDE estimation in RAPTOR.
3. Demonstrating combined mesh and model error estimation in RAPTOR.

In parallel, we extended VMS estimators to a Finite Volume framework for thermally coupled Navier-Stokes equations.

Phase II Progress: MDE formulation

Primary focus: formulating a minimally intrusive extension of RAPTOR:

- An interpolator was implemented in RAPTOR that projects coarse mesh solution into finer meshes.
- Non-linear terms of the LES equations were written to output files.
- The output files were read and interpolated as a first step for the down-scaling procedure.
- Need to solve a forced heat equation [in progress].
- The error source term is to be injected into LES equation to solve for corrected (nudged) solution [in progress]

Phase II Progress: Demonstrate MDE estimation

- We restricted our attention to scalar fields, which enabled us to demonstrate the methodology for P1 without modifying RAPTOR.
- Density field was chosen as solving a forced heat equation would not be required.

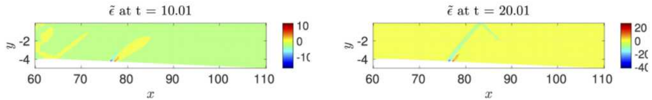

- Generated a number of realizations of MDE for density field at different grid and time-step levels.

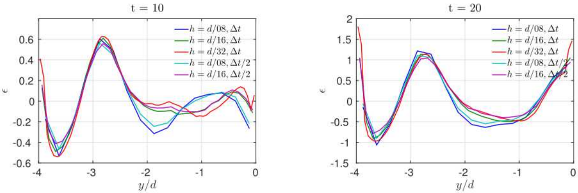

Phase II Progress: Demonstrate combined MDE/ME estimation

- We conducted an investigation on the possibility of combining ME/MDE estimates in the LES context.
- ME posteriors may exhibit a non-trivial dependence on mesh resolution.

→ Need to analyze ME and MDE independently, so that combined impact may be suitably assessed.

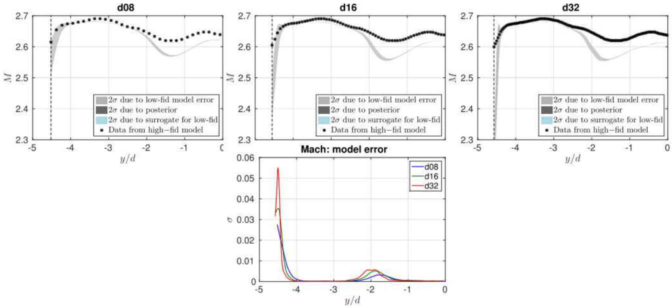

Phase II Progress: Extended VMS to FV framework

In a FE framework, for a given element $K \in \mathcal{T}_h$, we can obtain a definition of the error estimator, η_K^{VMS} for the Boussinesq equations:

$$\eta_K^{\text{VMS}} := \text{meas}(K)^{1/2} \boldsymbol{\tau}_{m,L^2}^{+} \|\mathcal{R}_m(\bar{\mathbf{U}})\|_{\mathbf{L}^\infty(K)}$$

with $\mathcal{R}_m(\bar{\mathbf{U}})$ the momentum equation residual

$$\mathcal{R}_m(\bar{\mathbf{U}}) = \mathbf{f} + \alpha \mathbf{g} \theta_0 - \left[\partial_t \bar{\mathbf{u}} - \nu \Delta \bar{\mathbf{u}} + \bar{\mathbf{u}} \cdot \nabla \bar{\mathbf{u}} + \nabla \bar{p} + \alpha \mathbf{g} \bar{\theta} \right].$$

In a FV context, we assume that the residual is piecewise constant. Thus, the $\mathbf{L}^\infty$-norm of the constant residual is computed as

$$\|\mathcal{R}_m(\bar{\mathbf{U}})\|_{\mathbf{L}^\infty(K)} = \left|\mathcal{R}_m(\bar{\mathbf{U}})\right|_K = \left| \frac{1}{\text{meas}(K)} \int_K \mathcal{R}_m(\bar{\mathbf{U}}) d\Omega \right|.$$

We evaluate the integral by computing the fluxes between FV cells.

Phase II Progress: Extended VMS to FV framework

- Extended the VMS error estimator for thermally stratified flow
- Defined the standard version of the VMS error estimator in a Finite Volume framework
- The applicability of the VMS error estimators for a FV computation has been successfully demonstrated for the Rayleigh-Bénard problem

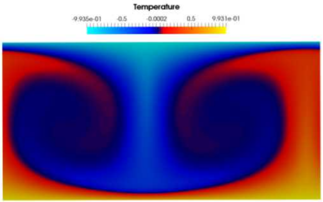

(a) Temperature

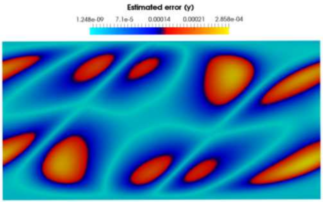

(b) Error y-component

Outline

OUU Progress

DAKOTA+(S)NOWPAC

P2 OUU Target: SNOWPAC DFO + Dakota MLMC

- Testing, refinement (scaling, bounds), parallelism
- Expand error estimation for OUU robustness / reliability targets
- Harden for small sample sizes (e.g., 5 - 2 fail) $\rightarrow$ unbiased multilevel estimates for population-based central moments to order 4

Error estimation:

- MC std errors are well developed
- Multilevel std errors are more involved (e.g., std error of variance)

$$
\begin{aligned}
\mathsf{Var}(\hat{\sigma}^2_L) &= \sum_{\ell=0}^{L} \mathsf{Var}(\hat{P}^2_\ell) - \mathsf{Var}(\hat{P}^2_{\ell-1}) - 2\mathrm{Cov}(\hat{P}^2_\ell, \hat{P}^2_{\ell-1}) \\
\mathsf{Var}(\hat{P}^2_\ell) &= \frac{1}{N_\ell}\left(\mu_{4,\ell} - \mathsf{Var}^2(Q_\ell)\right) + \frac{2}{N_\ell(N_\ell-1)}\mathsf{Var}^2(Q_\ell) \\
\mathrm{Cov}(\hat{P}^2_\ell, \hat{P}^2_{\ell-1}) &= \frac{1}{N_\ell}\left(\mathbb{E}\left[P^2_\ell P^2_{\ell-1}\right] - \mathsf{Var}(Q_\ell)\mathsf{Var}(Q_{\ell-1})\right) + \frac{1}{N_\ell(N_\ell-1)}\left(\mathbb{E}\left[Q_\ell Q_{\ell-1}\right] - \mathbb{E}\left[Q_\ell\right]\mathbb{E}\left[Q_{\ell-1}\right]\right)^2 \\
\mathbb{E}\left[P^2_\ell P^2_{\ell-1}\right] &= \mathbb{E}\left[Q^2_\ell Q^2_{\ell-1}\right] - 2\mathbb{E}\left[Q_{\ell-1}\right]\mathbb{E}\left[Q^2_\ell Q_{\ell-1}\right] + \mathbb{E}^2\left[Q_{\ell-1}\right]\mathbb{E}\left[Q^2_\ell\right] - 2\mathbb{E}\left[Q_\ell\right]\mathbb{E}\left[Q_\ell Q^2_{\ell-1}\right] \\
&+ 4\mathbb{E}\left[Q_\ell\right]\mathbb{E}\left[Q_{\ell-1}\right]\mathbb{E}\left[Q_\ell Q_{\ell-1}\right] + \mathbb{E}^2\left[Q_\ell\right]\mathbb{E}\left[Q^2_{\ell-1}\right] - 3\mathbb{E}^2\left[Q_\ell\right]\mathbb{E}^2\left[Q_{\ell-1}\right]
\end{aligned}
$$

OUU Progress

DAKOTA+(S)NOWPAC

Error estimation (continued):

- Multilevel std error for std deviation (no closed form for single level)
  - Normally-distributed *population*

$$SE(\hat{\sigma}) = \frac{\hat{\sigma}}{\sqrt{2(N-1)}}$$

  - Function of a normally-distributed *estimator* (Delta Method)

$$SE(\hat{\sigma}) = \frac{1}{2\hat{\sigma}} \sqrt{\frac{1}{N}\left(\mu_4 + \frac{3-N}{N-1}(\sigma^2)^2\right)}$$

- Additional need for unbiased multilevel (4^{th}) central moments

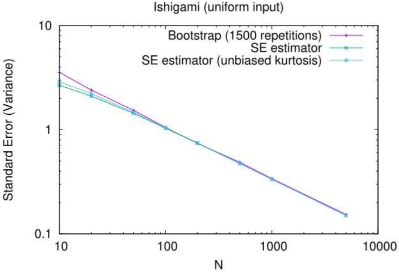

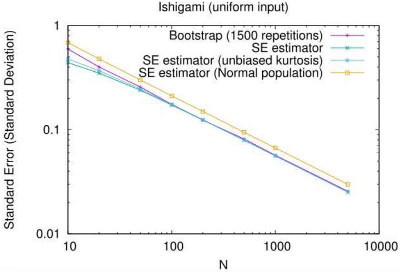

OUU Progress

AFRL WPAFB site visit → finalize OUU formulation:

$$\begin{aligned} \max \quad & \mathbb{E}[\eta_{\text{thermal}}] \\ s.t. \quad & p[\phi_{\text{burn}} \le 0.7] \le .01 \\ & p[x_{\text{shocktrain}} \le 4\ in] \le .01 \\ & p[\Delta_{\text{press}} \ge .05 * \mu_{\text{press}}] \le .01 \end{aligned}$$

P2 OUU demo in progress: MLMC analyses at initial design points

	$\mathbb{E}[\eta_{\text{thermal}}]$	$\mathbb{E}[\phi_{\text{burn}}]$	$\mathbb{E}[x_{\text{shocktrain}}]$
Nominal	0.018494 $\pm$ 3.7542e-08	0.10151 $\pm$ 1.1309e-06	74.744 $\pm$ 0.
Δd_1	0.018804 $\pm$ 5.6828e-08	0.098653 $\pm$ 1.5642e-06	74.744 $\pm$ 0.
Δd_2	0.018682 $\pm$ 6.1177e-08	0.10254 $\pm$ 1.8430e-06	74.744 $\pm$ 0.
Δd_3	0.018739 $\pm$ 1.2493e-07	0.10285 $\pm$ 3.7635e-06	26.033 $\pm$ 133.06
Δd_4	0.018434 $\pm$ 2.2739e-08	0.10117 $\pm$ 6.8503e-07	74.744 $\pm$ 0.
Δd_5	0.019003 $\pm$ 2.8257e-08	0.10430 $\pm$ 8.5124e-07	21.637 $\pm$ 95.363
Step 1	pending	pending	pending

Table: History to date for statistical QoIs from MLMC analyses in P2 OUU for design variables d = { global equiv ratio, fuel ratio$_{1:2}$, inj locn$_1$, inj locn$_2$, inj angle$_1$ }.

OUU Impact

P1 (jet in cross flow):

- Have demonstrated viability of LES-based OUU for P1
  $\rightarrow$ Dakota: PCBDO w/ combined exp, Multifidelity TRMM
  $\rightarrow$ SNOWPAC: direct coupled w/ RAPTOR

P2 (scramjet):

- Currently generating OUU results for P2
  $\rightarrow$ integrating stochastic DFO with multilevel-multifidelity UQ
  $\rightarrow$ investigating design considerations recommended by AFRL SMEs
  $\rightarrow$ ultimately expect new design insights from HF LES-based design

Phase II planned work:

- Increase resolution as enabled by large-scale HPC: include 3D, increase FTTs, tighten ML tolerances, include chance constraints, etc.
- Integrate emerging capabilities from TAs 1,2 $\rightarrow$ comprehensive OUU

Outline

Closure

Phase II work in progress with Scramjet code

- Routine RAPTOR P2 runs – currently 2D
- Addressing high-dimensionality and MLMF challenges in P2-2D
  - GSA-PC-CS-ML, ASQ
  - Basis adaptation and manifold discovery
- Work on data-informed subspaces, model, and mesh error
- OUU demonstrations in P2

Targeting additional computational resources – especially for 3D P2

- We have access to multiple SNL machines
  - each with several thousand cores
- We are exploring DOD resources